J|A|C|S
ARTICLES
Published on Web 12/16/2005

# Infrared Spectroscopy of Phenylalanine Ag(I) and Zn(II) Complexes in the Gas Phase

Nick C. Polfer,[†] Jos Oomens,[†] David T. Moore,[†,||] Gert von Helden,[‡] Gerard Meijer,[‡] and Robert C. Dunbar*[,§]

*Contribution from the FOM-Institute for Plasmaphysics Rijnhuizen, Edisonbaan 14, NL-3439 MN Nieuwegein, The Netherlands, Fritz-Haber-Institut der Max-Planck-Gesellschaft, Faradayweg 4-6, D-14195 Berlin, Germany, and Chemistry Department, Case Western Reserve University, Cleveland, Ohio 44106*

Received July 22, 2005; E-mail: rcd@po.cwru.edu

***Abstract:*** Infrared multiple-photon dissociation (IR-MPD) spectroscopy has been applied to singly-charged complexes involving the transition metals $Ag^+$ and $Zn^{2+}$ with the aromatic amino acid phenylalanine. These studies are complemented by DFT calculations. For $[Phe+Ag]^+$ the calculations favor a tridentate charge solvation N/O/ring structure. The experimental spectrum strongly supports this as the predominant binding geometry and, in particular, rules out a significant presence of the salt-bridge conformation. $Zn^{2+}$ forms a deprotonated dimer complex with Phe, $[Zn+Phe_2-H]^+$, in which the +2 oxidation state serves as a useful biomimetic model for zinc protein sites. A number of low-energy conformations were located, of which the lowest-energy conformer predicted by the calculations involves a Phe ligand deprotonated on the carboxylic acid, while the other Phe ligand is in the tridentate charge solvation conformation. The calculated IR spectrum of this conformer gives a close fit to the experimental spectrum, strongly supporting this as the predominant binding geometry. This most stable calculated complex is characterized by N/ O/ring metal chelation with a tetrahedral-type coordination core of $Zn^{2+}$ to N and O of both ligands. Another similar tightly chelated structure shows a square-planar-type coordination core, but this structure is computed to be less stable and gives a less satisfactory match to the experimental spectrum. This preference for the tetrahedral geometry of the Lewis-basic atomic ligands parallels the common Zn(II) coordination geometry in proteins. The number of clearly identifiable peaks resolved in the IR-MPD spectra as well as the much-improved matches between the observed spectra and the DFT-calculated spectra of the most stable geometries compared to previous studies are noteworthy for systems of this size and complexity. These results demonstrate that IR spectroscopy of transition metal−amino acid complexes in combination with DFT calculations is a very powerful structural tool, readily applicable to biomimetic systems that model, for example, the reaction centers of proteins in the solvent-free environment. In addition, we present a novel ion-capturing method for Fourier transform ion cyclotron resonance mass spectrometry which removes the necessity of a buffer gas pulse, while allowing ion trapping at moderate voltages with apparently reduced collisional excitation of the ions.

## Introduction

The role of transition metals in biology can hardly be overemphasized. A full third of all structurally characterized proteins are metalloproteins, in many of which transition metals are critical for the catalytic and structural properties of the proteins.[1] Zinc is among the most abundant transition metals in the cytoplasm ($10^5$ atoms per cell), and its role in the gene-regulatory Zn finger proteins is well documented.[2−4] Zn is especially important in the structural organization of proteins.[4] As opposed to other transition metals (e.g., Fe, Cu) Zn exists as a divalent cation, $Zn^{2+}$, with a filled d electronic shell in physiological conditions. The electronic configuration of $Zn^{2+}$ explains its inertness to redox reactions and hence rationalizes the limited catalytic activity of Zn in proteins, as for example in carbonic anhydrase.[5] $Zn^{2+}$ is a soft Lewis acid due to a vacant s orbital, which allows strong interaction with a variety of ligands, including sulfur from cysteine, nitrogen from histidine, and oxygen from glutamate, aspartate, and water. Another consequence of the filled d shell is the absence of a geometry-dependent ligand field stabilization energy (LFSE). This also explains the high preference for $Zn^{2+}$ to form tetrahedral binding sites in proteins.[4,6−8] Whereas transition metals with partially

[†] FOM-Institute for Plasmaphysics Rijnhuizen.
[‡] Fritz-Haber-Institut der Max-Planck-Gesellschaft.
[§] Case Western Reserve University.
[||] Present address: Chemistry Department, University of California Berkeley, Berkeley, CA 94720.

(1) Finney, L. A.; O'Halloran, T. V. *Science* **2003**, *300*, 931−936.
(2) Klug, A.; Rhodes, D. *Trends Biochem. Sci.* **1987**, *12*, 464−469.
(3) Schwabe, J. W. R.; Klug, A. *Nat. Struct. Mol. Biol.* **1994**, *1*, 345−349.
(4) Berg, J. M.; Shi, Y. *Science* **1996**, *271*, 1081−1085.
(5) Keilin, D.; Mann, T. *Biochem. J.* **1940**, *34*, 1163−1176.
(6) Regan, L.; Clarke, N. D. *Biochemistry* **1990**, *29*, 10878−10883.
(7) Klemba, M.; Regan, L. *Biochemistry* **1995**, *34*, 100094−110100.
(8) Venkataraman, D.; Du, Y.; Wilson, S. R.; Hirsch, K. A.; Zhang, P.; Moore, J. S. *J. Chem. Educ.* **1997**, *74*, 915−918.

filled d shells lose LFSE upon going from an octahedral $M(H_2O)_6$ arrangement in solution to a tetrahedral site in a protein, this is not the case for $Zn^{2+}$.[9] For tetrahedral binding sites with cysteine and histidine ligands in proteins, the Zn binding affinity is 1−2 orders of magnitude higher than that for other divalent metals. Despite the high binding strength, $Zn^{2+}$ is relatively labile, undergoing rapid ligand exchange reactions[10] and exchanging from protein binding sites except for sterically hindered sites.[11]

Like zinc, silver only assumes the $d^{10}$ electronic configuration in physiological conditions, existing as $Ag^+$. Except for some antimicrobial activity,[12,13] silver is biologically relatively inactive. Nevertheless, in addition to its indirect interest as a model for tightly bound metal ions in general, the binding of $Ag^+$ to amino acids and peptides is directly interesting in view of the interesting fragmentation chemistry of argentiated peptides by collisional-induced dissociation (CID).[14−16] The fragmentation of $Ag^+$-tagged phenylalanine, $[Phe+Ag]^+$, also shows different fragmentation behavior compared to alkali metals or other transition metals.[17] The structure of $[Phe+Ag]^+$ was inferred to be a tightly coordinated complex from density functional theory (DFT) calculations, which was supported by hydration and MeOH addition reactions to $[Phe+Ag]^+$ in an ion trap.[18]

Of particular interest are the structural and catalytic properties of transition metals in metalloproteins. For example, the detailed mechanistic pathways and transition states of copper proteins are only partially understood[19] and often rely on the generation of stable intermediates that can be characterized by X-ray crystallography.[20,21] The conclusions from such studies can be ambiguous, and often further studies are required to confirm the mechanistic implications.[22] An alternative strategy for investigating the mechanism in protein active sites involves the study of smaller model systems that only include the transition metal and chelating ligands and can hence mimic the structure and function of the active site.[23,24] Such systems are also known as biomimetics, and their structural study is usually carried out in the condensed phase using X-ray crystallography, FTIR, and electron paramagnetic resonance (EPR).[25−27] Due to the relatively small size of biomimetics, such complexes lend themselves to structural elucidation in the absence of solvent or other effects (i.e., in the gas phase) by infrared spectroscopy, which can be directly compared to condensed-phase structures. This enables a separation of the intra- and intermolecular forces on the active site conformation. Further, the theoretical study of such systems with DFT calculations has expanded considerably in the past few years and can yield important insights into the reactive mechanisms of protein catalytic sites.[28−31] It is necessary to have experimental tools, such as infrared spectroscopy, that can validate the theoretical models. Illustrating one aspect of such possibilities for transition metals with partially filled d shells, it has been shown that infrared spectroscopy can help elucidate which DFT functional gives the most accurate thermochemical predictions.[32]

Due to the charge on the metals in their normal oxidation states, the metal-containing centers of many biologically interesting metal−ligand complexes are inherently charged. The mass-spectrometric study of charged complexes as models for biological metal centers is thus inherently relevant. To investigate such species, it is attractive to use spectroscopic approaches, in particular infrared (IR) spectroscopy, as more direct and definitive structural probes than the indirect reactivity and fragmentation probes that have mostly been the only available approaches for gas-phase ionic molecules. Direct absorption spectroscopy on ions under mass-spectrometric control is challenging, due to the low ion density that can be maintained in the face of the Coulombic repulsion between gas-phase ions. Used as an "action spectroscopy" strategy[33] in place of direct IR absorption spectroscopy, infrared multiple-photon dissociation (IR-MPD)[34] has been successfully implemented as an effective alternative strategy for achieving IR spectroscopic study of a number of metal−ligand complexes.[32,35−39] IR-MPD relies on the resonant noncoherent absorption of typically hundreds of photons to reach high internal energies where one or more dissociation pathways are usually accessible, for which powerful laser systems are essential. Free electron lasers (FEL) have proven to be well-suited for this task and have the capability of continuous wavelength-tunability over a very wide range (3−250 $\mu$m).

The metal−biomolecule complexes studied so far by infrared spectroscopy in this way have been limited to complexes of


(9) Berg, J. M.; Merkle, D. L. *J. Am. Chem. Soc.* **1989**, *111*, 3759−3761.
(10) Eigen, M. *Pure Appl. Chem.* **1963**, *6*, 97−115.
(11) Blindauer, C. A.; Polfer, N. C.; Keiper, S. E.; Harrison, M. D.; Robinson, N. J.; Langridge-Smith, P. R. R.; Sadler, P. J. *J. Am. Chem. Soc.* **2003**, *125*, 3226−3227.
(12) Nomiya, K.; Onoue, K.-I.; Kondoh, Y.; Kasuga, N. C.; Nagano, H.; Oda, M.; Sakuma, S. *Polyhedron* **1995**, *14*, 1359−1367.
(13) Nomiya, K.; Kondoh, Y.; Nagano, H.; Oda, M. *J. Chem. Soc., Chem. Commun.* **1995**, *1995*, 1679−1680.
(14) Lee, V. W.-M.; Li, H.; Lau, T.-C.; Siu, K. W. M. *J. Am. Chem. Soc.* **1998**, *120*, 7302−7309.
(15) Chu, I. K.; Guo, X.; Lau, T.-C.; Siu, K. W. M. *Anal. Chem.* **1999**, *71*, 2364−2372.
(16) Chu, I. K.; Shoeib, T.; Guo, X.; Rodriquez, F.; Lau, T.-C.; Hopkinson, A. C.; Siu, K. W. M. *J. Am. Soc. Mass Spectrom.* **2001**, *12*, 163−175.
(17) Talaty, E. R.; Perera, B. A.; Gallardo, A. L.; Barr, J. M.; Van Stipdonk, M. J. *J. Phys. Chem. A* **2001**, *105*, 8059−8068.
(18) Perera, B. A.; Gallardo, A. L.; Barr, J. M.; Tekarli, S. M.; Anbalagan, V.; Talaty, E. R.; Van Stipdonk, M. J. *J. Mass Spectrom.* **2002**, *37*, 401−413.
(19) Lewis, E. A.; Tolman, W. B. *Chem. Rev.* **2004**, *104*, 1047−1076.
(20) Prigge, S. T.; Eipper, B. A.; Mains, R. E.; Amzel, L. M. *Science* **2004**, *304*, 864−867.
(21) Tocheva, E. I.; Rosell, F. I.; Mauk, A. G.; Murphy, M. E. P. *Science* **2004**, *304*, 867−870.
(22) Aboelella, N. W.; Reynold, A. M.; Tolman, W. B. *Science* **2004**, *304*, 836−837.
(23) Vahrenkamp, H. *Acc. Chem. Res.* **1999**, *32*, 589−596.
(24) Kimura, E. *Acc. Chem. Res.* **2001**, *34*, 171−179.
(25) Beretta, M.; Bouwman, E.; Casella, L.; Douziech, B.; Driessen, W. L.; Gutierrez-Soto, L.; Monzani, E.; Reedijk, J. *Inorg. Chem.* **2000**, *310*, 41−50.
(26) Prisner, T.; Rohrer, M.; MacMillan, F. *Annu. Rev. Phys. Chem.* **2001**, *52*, 279−313.
(27) Gamez, P.; Koval, I. A.; Reedijk, J. *Dalton Trans.* **2004**, *2004*, 4079−4088.
(28) Siegbahn, P. E. M.; Blomberg, M. R. A. *Annu. Rev. Phys. Chem.* **1999**, *50*, 221−249.
(29) Cheng, Y.; Zhang, Y.; McCammon, J. A. *J. Am. Chem. Soc.* **2005**, *127*, 1553−1562.
(30) Marino, T.; Russo, N.; Toscano, M. *J. Am. Chem. Soc.* **2005**, *127*, 4242−4253.
(31) Sousa, S. F.; Fernandes, P. A.; Ramos, M. J. *Biophys. J.* **2005**, *88*, 483−494.
(32) Oomens, J.; Moore, D. T.; von Helden, G.; Meijer, G.; Dunbar, R. C. *J. Am. Chem. Soc.* **2004**, *26*, 724−725.
(33) Wing, W. H.; Ruff, G. A.; Lamb, J. W. E.; Spezeski, J. J. *Phys. Rev. Lett.* **1976**, *36*, 1488−1491.
(34) Bagratashvili, V. N.; Letokov, V. S.; Makarov, A. A.; Ryabov, E. A. *Multiple Photon Infrared Laser Photophysics and Photochemistry*; Harwood: Chichester, U.K., 1985.
(35) Cabarcos, O. M.; Weinheimer, C. J.; Lisy, J. M. *J. Chem. Phys.* **1999**, *110*, 8429−8435.
(36) Moore, D. T.; Oomens, J.; Eyler, J. R.; Meijer, G.; von Helden, G.; Ridge, D. P. *J. Am. Chem. Soc.* **2004**, *126*, 14726−14727.
(37) Kapota, C.; Lemaire, J.; Maitre, P.; Ohanessian, G. *J. Am. Chem. Soc.* **2004**, *126*, 1836−1842.
(38) Polfer, N.; Paizs, B.; Snoek, L. C.; Compagnon, I.; Suhai, S.; Meijer, G.; von Helden, G.; Oomens, J. *J. Am. Chem. Soc.* **2005**, *127*, 8571−8579.
(39) Moore, D. T.; Oomens, J.; Eyler, J. R.; von Helden, G.; Meijer, G.; Dunbar, R. C. *J. Am. Chem. Soc.* **2005**, *127*, 7243−7254.

the alkali metals sodium[37] and potassium.[38] In those studies, one of the main purposes was to determine whether a charge solvation (CS) or salt bridge (SB) complex was formed. Infrared studies of transition metal−biomolecule complexes in the gas phase have not been attempted to our knowledge.

Electrospray ionization (ESI)[40] is a convenient tool to generate metal-coordinated complexes.[41] Here, singly-charged phenylalanine complexes with the transition metals $Ag^+$ and $Zn^{2+}$ are investigated using infrared photofragment spectroscopy. For the first IR-spectroscopic study of transition metal−amino acid complexes, these two ions seemed appropriate in that their filled-shell $d^{10}$ character makes them comparable in some respects to previous and ongoing studies with alkali metal ions, along with the fact that electrospray production of their complexes presents less difficulty than those of more reactive open-shell transition metal ions. The $Ag^+$ ion studied here is in the normal oxidation state to serve as a model for biological monocations. It is quite similar in size to $Na^+$, as indicated by the computational results below, and offers an interesting comparison with previous gas-phase spectroscopy of alkali metal ion complexes. It is less straightforward to mimic condensed-phase $Zn^{2+}$ using gas-phase conditions, since a gas-phase $Zn^{2+}$ carries a full +2 charge whose very large Coulomb interactions with ligands cannot be expected to give a realistic analogy to condensed-phase conditions. The deprotonated dimer complex of $Zn^+$ studied here corresponds to zinc in the +2 oxidation state, but carrying only a +1 charge, making it a more realistic mimic for biocomplexes of Zn(II).[42]

## Experimental and Calculational Section

**Experimental.** The experiments were conducted in a laboratory-constructed Fourier transform ion cyclotron resonance mass spectrometer (FTICR-MS),[43] computer-controlled using the Modular ICR Data Acquisition System (MIDAS)[44] developed at the National High Magnetic Field Laboratory in Tallahassee, FL. Phenylalanine was made up at a 1 mM concentration in a MeOH/$H_2O$ (80:20) solution; AgCl and $ZnCl_2$ were added at a concentration of 0.5 mM. These solutions were syringe-infused into a commercial ESI source (Z-Spray, Micromass, U.K.). The ions were accumulated in a storage hexapole (∼500 ms) before pulse extraction through a quadrupole deflector and an rf octopole ion guide into the Penning trap of the FTICR-MS. Capturing ions in the trap was effected by a novel experimental method, which is further detailed below. The ions were left to cool by radiative emission for 350 ms, followed by mass isolation and infrared irradiation with 20−80 macropulses (2−8 s ion storage at 10-Hz macropulse repetition rate) from the Free Electron Laser for Infrared eXperiments (FELIX).[45] FELIX produces high-energy (60-mJ) macropulses of 1-ns-spaced micropulses for a duration of about 5 $\mu$s. Optical access to the trap was enabled by a ZnSe window on the rear side of the instrument. The laser beam was focused with an elliptical mirror into the Penning trap, of which both cylindrical copper excitation electrodes were polished to create a multipass cell (6−7 passes through the ion cloud).

**IR-MPD Spectroscopy.** As the experimental method relies on the absorption of multiple, typically tens to hundreds of infrared photons, the interpretation of the spectra needs some special attention. First of all, it is important to note that multiple photon absorption occurs in an incoherent fashion, so that highly nonlinear power dependencies, such as encountered in coherent multiphoton absorption processes, are largely avoided here.[34,46,47] Such an incoherent absorption process assumes complete randomization of the energy pumped into the molecule by fast intramolecular vibrational redistribution (IVR). Nonetheless, the measured band positions and widths are affected by the excitation process in an intricate way that is mainly governed by the molecular anharmonicity parameters, which in principle are different for each vibration. The actual observed fragmentation efficiency depends in addition on various experimental parameters such as laser fluence and focal volume (changing with wavelength) relative to the ion cloud size, initial internal energy (i.e., temperature), the time scale of the experiment, as well as on the proximity of other bands in the spectrum and on the dissociation threshold. Although models have been developed to investigate these effects, the precise imprint of the IR-MPD process on the spectrum of a particular molecule remains difficult to estimate, especially since anharmonicity parameters are generally not known.

We have extensively studied the IR-MPD spectra of a number of polyaromatic cations, for which good matrix isolation spectra are available for comparison and for which very unambiguous DFT calculations have been performed. This study[48] has empirically shown that (a) relative band intensities (after applying a linear power correction) are in fair agreement with those of linear absorption spectra, that (b) red-shifts due to anharmonicity are typically on the order of 5−20 $cm^{-1}$, i.e., a few percent, and that (c) line widths, which are mainly determined by the IR-MPD process (i.e., not by the laser bandwidth of ∼5 $cm^{-1}$), are on the order of 30 $cm^{-1}$, although they can be quite molecule specific. In case of very strongly bound species, higher than linear power dependencies have been observed,[49] and in addition, closely spaced bands may give rise to somewhat abnormal band intensities as well.[48] These findings led us to apply a linear laser power correction to the measured fragmentation yield to account for the variations in pulse energy with wavelength.

As noted above, the internal energy of the ions is one of the factors influencing the line width of the observed infrared bands, and therefore the commonly used method of collisionally stopping the ions in the ICR cell may give rise to a lower spectral resolution. Below we describe a novel method of capturing the ions produced in external sources that avoids collisional heating effects.

**Ion Capture Method.** To avoid the magnetic mirror effect, ions produced in an external ion source often traverse the region between low and high magnetic fields in radio frequency (rf) ion guides that are based on multipoles or stacked ring electrodes. In these devices, the ions travel with a kinetic energy of typically between 25 and 100 eV in order to achieve effective injection into the high magnetic field region. To capture the ions in the Penning trap of the FTICR-MS, this kinetic energy needs to be removed upon entering the ICR cell, and several methods to this end have been developed.[50] One of the most common methods is to inject a pulse of buffer gas to collisionally dissipate the kinetic energy. Drawbacks are an increase in internal energy, possibly resulting in fragmentation of the ions, and in addition, a pumping delay on the order of one or more seconds is necessary to return to the low pressures required for detection of the ICR transient. For pulsed ion injection, gated trapping can be applied, which simply gates the voltage on the front trapping plate down when the ion bunch arrives, while the rear trapping plate is biased high enough to stop the

(40) Fenn, J. B.; Mann, M.; Meng, C. K.; Wong, S. F.; Whitehouse, C. M. *Science* **1989**, *246*, 64−71.
(41) Schalley, C. A. *Int. J. Mass Spectrom.* **2000**, *194*, 11−39.
(42) Deerfield, D. W.; Carter, C. W., Jr.; Pederson, L. G. *Int. J. Quantum Chem.* **2001**, *83*, 150−165.
(43) Valle, J. J.; Eyler, J. R.; Oomens, J.; Moore, D. T.; van der Meer, A. F. G.; von Helden, G.; Meijer, G.; Hendrickson, C. L.; Marshall, A. G.; Blakney, G. T. *Rev. Sci. Instrum.* **2005**, *76*, 23103/1−23103/7.
(44) Senko, M. W.; Canterbury, S. H.; Marshall, A. G. *Rapid Commun. Mass Spectrom.* **1996**, *10*, 1839−1844.
(45) Oepts, D.; van der Meer, A. F. G.; van Amersfoort, P. W. *Infrared Phys. Technol.* **1995**, *36*, 297−308.
(46) Black, J. G.; Yablonovitch, E.; Bloembergen, N.; Mukamel, S. *Phys. Rev. Lett.* **1977**, *38*, 1131−1134.
(47) Grant, E. R.; Schulz, P. A.; Sudbo, A. S.; Shen, Y. R.; Lee, Y. T. *Phys. Rev. Lett.* **1978**, *40*, 115−118.
(48) Oomens, J.; Tielens, A. G. G. M.; Sartakov, B. G.; von Helden, G.; Meijer, G. *Astrophys. J.* **2003**, *591*, 968−985.
(49) Oomens, J.; Sartakov, B. G.; Tielens, A. G. G. M.; Meijer, G.; von Helden, G. *Astrophys. J.* **2001**, *560*, L99−L103.
(50) Marshall, A. G. *Int. J. Mass Spectrom.* **2000**, *200*, 331−356.

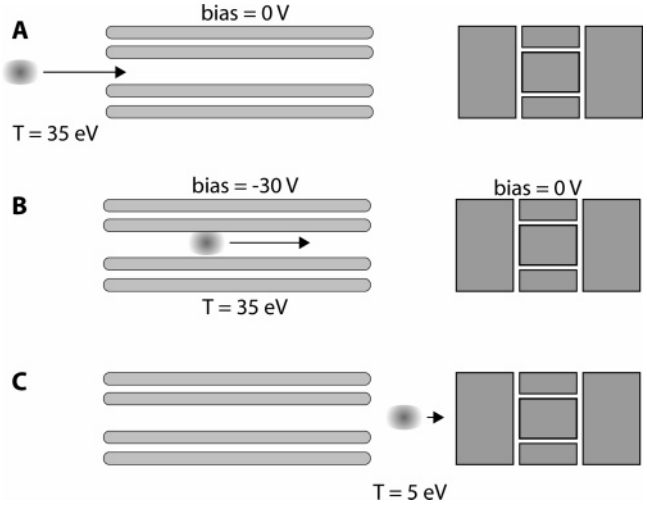


***Figure 1.*** Schematic sequence of events used to guide and trap externally generated ions in the ICR. (A) A bunch of ions extracted from an accumulation device with a kinetic energy of typically 35 eV is sent into a 1-m long rf-driven octopole ion guide. (B) Once inside the octopole, the dc bias on the octopole rods is abruptly switched to −30 V, thereby lowering the potential energy of ions. However, the ions' kinetic energy does not change since there is no dc potential gradient in the forward direction at any moment. (C) Upon leaving the octopole, the ground potential on the ICR cell (right) reduces the ions' kinetic energy to typically 5 eV so that they can be trapped easily. Note that the values given are typical and are actually optimized experimentally.

ions. However, trapping voltages of several tens of volts are required, which is impractical for subsequent ICR detection. Another method, known as side-kick, consists of creating a dc electric field perpendicular to the magnetic field lines so that ions are pushed away from the magnetic field axis, thereby converting the forward velocity into cyclotron and magnetron motion.[51] A disadvantage is the resulting off-axis distribution of ions in the cell, which may be corrected for by quadrupolar axialization; however, this requires again a pulse of buffer gas.[52] Note that several other methods have been developed as well.[53] Here we introduce a novel method of ion capturing, which overcomes some of the mentioned drawbacks. The method is similar to the potential switch introduced by Johnson and co-workers,[54] who used it to reference a pulse of ions to a different potential without changing its speed. We apply the "switch" to accomplish the opposite effect: changing the velocity of the ion beam without changing the (ground) reference potential.

The method is exemplified in Figure 1, where the sequence of events is depicted in panels A through C. A bunch of ions is extracted from the accumulation stage at a bias voltage of about 35 V into a 1-m long rf octopole at a dc bias of 0 V, thus giving the ions a kinetic energy of 35 eV (Figure 1A). Once the bunch is in the octopole, a dc bias voltage of about −30 V is superimposed on the rods carrying the rf drive voltage (Figure 1B). Since this bias is applied to the full length of all octopole rods, that is, there is no change whatsoever in the dc electric field along the axis of the ion guide, the ions do not gain or lose kinetic energy from this bias voltage switch; however, their potential energy is modified. Once the ions exit the octopole ion guide, they "see" the ICR cell, which is biased at ground potential, and by climbing the potential difference they slow to ∼5 eV (Figure 1C). As this happens within the high magnetic field region, the ion trajectories are restrained and de-focusing is not a concern. The ions can now conveniently be trapped by applying a moderate voltage on the ICR trapping plates.

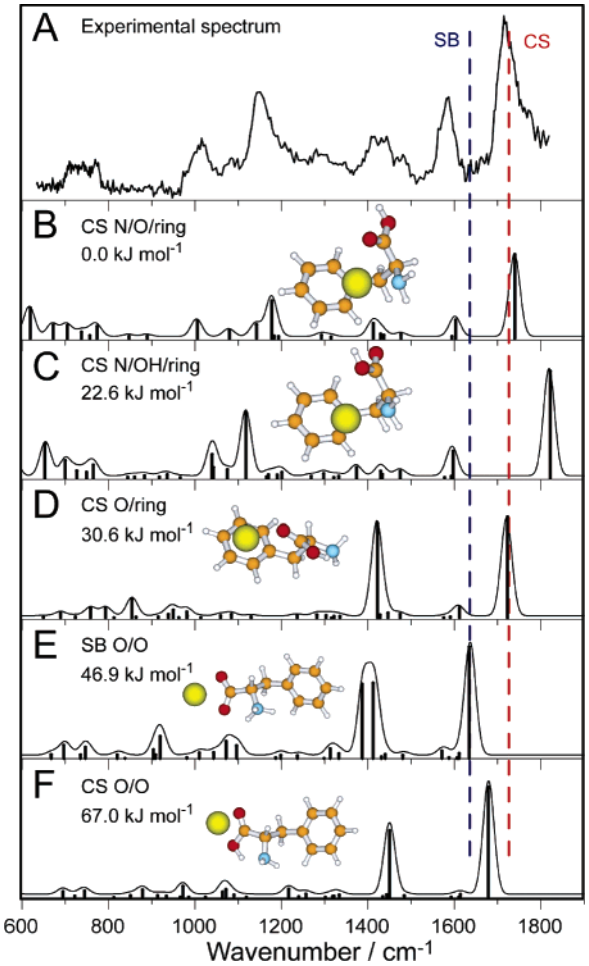


***Figure 2.*** (A) Experimental infrared spectrum of $[Phe+Ag]^+$, and relative energetics and spectra for optimized structures: (B) charge solvation N/O/ring, (C) charge solvation N/OH/ring, (D) charge solvation O/ring, (E) salt bridge O/O, and (F) charge solvation O/O. The dashed lines indicate the diagnostic vibrations for CS, carboxylic acid $\upsilon$(CO), and for SB, $\upsilon_{as}(CO_2^-)$.

This method combines the advantages of accelerating the ions from the source to ground, avoiding complicated shielding issues in the transfer region between the source and the ICR cell, and having the bias for the ICR cell at ground potential as well. Further, it does not require any inlet of buffer gas, reducing the internal energy of the ions as well as the duty cycle of the experiment. A relatively simple electronic circuit, triggered by a TTL pulse from the FTICR-MS data acquisition program, was constructed to apply the dc pulse to the octopole rods carrying the rf voltage at a frequency of about 1 MHz.

In terms of spectroscopic investigation of ions, the lower internal energy of the ions resulting from this method has the expected advantage that the IR-MPD spectra have more sharply resolved bands. While no direct comparison has been carried out to test this hypothesis, a comparison of $[Phe+Ag]^+$ (Figure 2 A) using the present method shows a marked spectral improvement to a previous study[38] involving $[Phe+K]^+$ using the commonly used gas-pulsing method. While there is no assurance that all ions are thermal at room temperature, the ions are unlikely to be subjected to significant heating in the ion generation or ion transfer; further, the ions are left to at least partially thermalize for hundreds of milliseconds in the ICR trap.

**Computational.** The DFT calculations were carried out using the Gaussian03 package.[55] For $[Phe+Ag]^+$, the plausible binding modes were assigned on the basis of previous experience with Phe complexes.[38,56] For $[Zn+Phe_2-H]^+$, a comprehensive structure search was

(51) Caravatti, P. U.S. Patent No. 4,924,089, May 8, 1990.
(52) Schweikhard, L.; Guan, S.; Marshall, A. G. *Int. J. Mass Spectrom.* **1992**, *120*, 71−83.
(53) Guan, S. H.; Pasa-Tolic, L.; Marshall, A. G. *Int. J. Mass Spectrom. Ion Processes* **1994**, *139*, 75−86.
(54) Posey, L. A.; Deluca, M. J.; Johnson, M. A. *Chem. Phys. Lett.* **1986**, *131*, 170−174.
(55) Frisch, M. J., et al. *Gaussian 03*; revision B3; Gaussian Inc.: Pittsburgh, PA, 2003.

not undertaken, but likely binding modes of both ligands were combined to give the set of putative structures for refinement. The structures were optimized and harmonic vibrational frequencies were calculated by DFT using the MPW1PW91 hybrid functional using a basis consisting of 6-311+G(d,p) on the metal ion and 6-31+G(d,p) on the other atoms. For Ag, the *sdd* relativistic effective core potential was used. To denote the metal−ligand chelation, the notation of Dunbar is employed.[57] The frequency spectra presented here are scaled by 0.965, as are all of the frequency values noted in the discussion and tables. A Gaussian convolution function with a fwhm of 30 $cm^{-1}$ is applied in plotting the theoretical spectra.

## Results and Discussion

**Silver.** *Mass Spectrometry.* ESI of the solution containing phenylalanine and AgCl gives rise to a $[Phe+Ag]^+$ complex (measured at *m*/*z* 272 and 274), which dissociates upon IR excitation via two different pathways: loss of neutral phenylalanine to yield the silver isotopes $^{107}Ag^+$ and $^{109}Ag^+$, as well as the fragments at *m*/*z* 227 and 229, which Talaty et al. have rationalized by the neutral losses of $NH_3$ and CO.[17] Note that no other dissociation channels were observed, in contrast to the CID studies of $[Phe+Ag]^+$.[17] The IR spectra of both dissociation pathways are almost identical, and they are summed to give the total IR-MPD spectrum in Figure 2A.

*$[Phe+Ag]^+$ CS or SB Conformation.* The infrared spectrum of $[Phe+Ag]^+$ is compared to the lowest-energy theoretical structures in Figure 2. The structures B, C, D, and F are charge-solvated (CS) conformation, while E has a salt-bridged (SB) conformation. Our calculations clearly predict a CS conformation, favoring the lowest-energy CS structure by a full 46.7 kJ $mol^{-1}$ relative to the lowest-energy SB structure (see Figure 2). Historically, Wyttenbach et al. made an interesting suggestion that zwitterionic SB structures would be favored for a number of cationized aromatic amino acids (including Phe) on the basis of proton affinities,[58] but this prediction has generally been discounted by more detailed theoretical calculations.[57,59]

As shown previously, the C═O stretch of an amino acid is a diagnostic vibration for the presence of a CS or SB conformation:[37,38] the antisymmetric stretch of the de-protonated carboxylate, $\upsilon_{as}(CO_2^-)$, indicative of SB, is calculated at ∼1640 $cm^{-1}$, whereas the carboxylic acid $\upsilon$(CO), indicative of CS, is calculated at higher frequencies for all modes of complexation, and in particular at ∼1740 $cm^{-1}$ for the most favored CS conformation. The complete absence of the expected SB peak in the observed spectrum rules out even a small fraction of the SB conformation. As further confirmation, only a weak feature is seen in the experimental spectrum at ∼1400 $cm^{-1}$, where the two intense umbrella modes of the $NH_3^+$ moiety, $\delta(NH_3^+)$, are expected for the SB structure (Figure 2E); the observed weak feature can be explained perfectly well by predicted modes in the CS structures. Thus, the experimental findings support the theoretical prediction that CS is strongly favored over SB. These results are also in agreement with the previous findings for $[Phe+K]^+$.[38]

*Assignment of $[Phe+Ag]^+$ CS Binding Geometry.* As shown in Figure 2, the theoretical studies have yielded a number of putative binding geometries for $[Phe+Ag]^+$ CS. The lowest-energy structure, CS N/O/ring, involves tridentate binding of the N, the carbonyl O, and the $\pi$-cloud of the aromatic ring (Figure 2B). The next-lowest-energy structure, CS N/OH/ring, is a similar tridentate structure in which the carbonyl O has exchanged places with the hydroxyl O (Figure 1C); this structure is already 22.6 kJ $mol^{-1}$ higher in energy. The next-lowest-energy structures, O/ring and O/O, and other higher-energy structures (not shown), are merely bidentate and are therefore even less favored energetically.

Clearly, the lowest-energy structure, CS N/O/ring, gives the closest fit to the experimental spectrum. In evaluating the acceptability of the fit between IR-MPD spectra and the predictions of DFT calculations at this level, it was useful in previous work[39] to compare the neutral IR absorption spectra of ligands in this size regime (using optimal frequency scaling factors) with predicted spectra: high-intensity peaks in one-to-one correspondence with the predicted high-intensity peaks gave agreement of peak positions generally within 10−15 $cm^{-1}$ and not usually worse than 25 $cm^{-1}$; however, relative peak intensities may be off by as much as a factor of 2. Compared with IR absorption spectra, IR-MPD spectra are expected to have somewhat greater frequency deviations; they may have substantially larger relative intensity deviations, for reasons discussed above. In this context, the agreement for the CS N/O/ring structure is highly satisfactory. It is the only structure for which all the calculated vibrational bands in the 700−1800 $cm^{-1}$ region are reproduced, and even the relative intensities are matched reasonably well. The bidentate structures CS O/ring and CS O/O are clearly less satisfactory in that they predict a very strong $\delta$(C−OH) mode at ∼1430 $cm^{-1}$, which is much weaker in the experimental spectrum, and at the same time they predict very little intensity at 1100−1200 $cm^{-1}$, where the experimental spectrum has a major feature. For the CS N/OH/ring structure, $\upsilon$(CO) is calculated to be blue-shifted to >1800 $cm^{-1}$, as a consequence of the absence of C═O metal chelation. The presence of a fraction of CS N/OH/ring cannot be definitively excluded, since the experimental frequency range up to ∼1800 $cm^{-1}$ did not span the predicted region of the characteristic C═O stretch for this isomer. However, the vibrational signatures between 1000 and 1500 $cm^{-1}$ for CS N/O/ring and CS N/OH/ring are significantly different, with the CS N/O/ring giving a noticeably better fit to the observed spectrum, so that the higher-energy CS N/OH/ring structure can be considered not to be a major fraction of the population. Consequently, we conclude that the bonding of this complex is definitely tridentate, and that between the two reasonable tridentate possibilities, the CS N/O/ring structure appears to be the dominant conformer even at room temperature. This is also in good agreement with DFT calculations[60] and $[Phe+Ag]^+$ gas-phase hydration studies by Perera et al.,[18] for which this tridentate structure rationalizes the steric hindrance to water addition.

The vibrational mode analysis of the experimental spectrum based on the best-fit theoretical structure CS N/O/ring is given in Table 1. Over this frequency range the vibrational modes are all essentially ligand-localized modes that are more or less perturbed by the presence of the metal ion. Thus, the discussion of several of the modes of metal-complexed Phe in the previous

(56) Gapeev, A.; Dunbar, R. C. *J. Am. Chem. Soc.* **2001**, *123*, 8360−8365.
(57) Dunbar, R. C. *J. Phys. Chem. A* **2000**, *104*, 8067−8074.
(58) Wyttenbach, T.; Witt, M.; Bowers, M. T. *J. Am. Chem. Soc.* **2000**, *122*, 3458−3464.
(59) Siu, F. M.; Ma, N. L.; Tsang, C. W. *J. Am. Chem. Soc.* **2001**, *123*, 3397−3398.
(60) Shoeib, T.; Hopkinson, A. C.; Siu, K. W. M. In *Proceedings of the 49th ASMS Conference on Mass Spectrometry and Allied Topics*; Chicago, IL, 2001; p A010370.pdf.

***Table 1.*** Assignment of Vibrational Bands in the Spectrum of $[Phe+Ag]^+$ in Figure 2A Based on the Calculated CS N/O/Ring Structure (Figure 2B)

| exptl ($cm^{-1}$) | calcd ($cm^{-1}$) | calcd intensity (km $mol^{-1}$) | assignment |
|---|---|---|---|
| 732 | 735 | 24 | aromatic $\delta_{oop}$(CH) |
| 769 | 771 | 45 | aromatic $\delta_{oop}$(CH) |
| 1016 | 1004 | 65 | $\delta_{oop}(NH_2)$ |
| 1085 | 1078 | 29 | aromatic $\upsilon$(CC) and $\delta_{ip}$(CH) |
| 1151 | 1141 | 51 | $\delta_{ip}$(COH)[a] |
| | 1176 | 137 | $\delta_{ip}$(COH)[a] |
| 1290 | 1291 | 13 | $\delta_{ip}$(COH)[a] |
| 1412 | 1411 | 56 | $\delta_{ip}$(COH)[a] |
| 1443 | 1428 | 17 | $CH_2$ scissoring |
| | 1436 | 13 | $CH_2$ scissoring |
| 1481 | 1476 | 15 | aromatic $\upsilon$(CC) and $\delta_{ip}$(CH) |
| 1587 | 1593 | 8 | aromatic $\upsilon$(CC) and $\delta_{ip}$(CH) |
| | 1602 | 68 | $NH_2$ scissoring |
| 1718 | 1739 | 303 | carboxylic acid $\upsilon$(CO) |

[a] $\delta_{ip}$(COH) always includes a large C−OH stretching component as well.

publication on $K^+$Phe[38] is equally applicable to the present system. The assignments of modes over the 1050−1800 $cm^{-1}$ range are similar. A few more frequencies are assigned in the present case (8 here compared with 6 in the previous $K^+$Phe work), as seemed justified by the lower congestion of the present spectrum.

The present spectrum extends to lower frequencies than the previous $K^+$Phe spectrum[24] (down to 630 $cm^{-1}$, compared with 1050 $cm^{-1}$). This allows the assignment of three additional bands observed below 1050 $cm^{-1}$ to out-of-plane bending modes. The free $NH_2$ out-of-plane bending mode is typically characterized by considerable anharmonicity and large deviations from harmonically calculated predictions, as was demonstrated for aniline[61] and some derivatives.[62] However, a nitrogen-coordinated metal ion constrains the vibration and greatly reduces the anharmonicity, as was demonstrated in the case of $Cr^+$ coordinated to aniline.[21] Similarly, in the present case there is no evidence of anharmonicity problems with the Phe $NH_2$ out-of-plane bending vibration, $\delta_{oop}(NH_2)$, seen at 1016 $cm^{-1}$, where the agreement between experiment and theory appears to be good.

*Comparison of $[Phe+Ag]^+$ to Alkali-Metal-Tagged Phe Complexes.* The differences in energy between the lowest-energy CS and SB structures are 77,[59] 10.1,[38] and 46.9 kJ $mol^{-1}$ for $Na^+$-, $K^+$-, and $Ag^+$-tagged Phe. In principle, a metal cation could favor the SB over the CS conformation due to the electrostatic stabilization of the negative charge on the carboxylate group.[63] Among these three metal ions it appears that $K^+$ comes the closest to rendering the SB conformation more stable than the CS conformation. This is in accord with computational findings by Marino et al. that the salt bridge form of proline-bound alkali metals becomes progressively more stable with increasing alkali metal size,[63] and also the similar results of Jockusch et al. for arginine-bound alkali metal ions.[64] However, in the Phe case the CS conformation remains the most stable, as has now been spectroscopically confirmed for both $K^+$ and $Ag^+$.

***Table 2.*** Comparison of Metal Chelation Atomic Distances in N/O/Ring Tridentate Structures for $[Phe+Na]^+$, $[Phe+K]^+$, and $[Phe+Ag]^+$ in angstroms

| | $[Phe+Na]^+$[a] | $[Phe+Na]^+$[b] | $[Phe+K]^+$[a] | $[Phe+K]^+$[b] | $[Phe+K]^+$[c] | $[Phe+Ag]^+$[d] |
|---|---|---|---|---|---|---|
| M···N | 2.46 | 2.45 | 2.91 | 2.90 | 2.94 | 2.38 |
| M···O | 2.31 | 2.30 | 2.68 | 2.66 | 2.68 | 2.49 |
| M···$\pi$ | 2.60 | 2.62 | 3.04 | 3.02 | 3.07 | 2.42 |

[a] Ref 54. [b] Ref 62. [c] Ref 38. [d] This work.

***Table 3.*** Binding Enthalpies for Metal−Phe Complexes: $[Phe+Na]^+$, $[Phe+K]^+$, and $[Phe+Ag]^+$ in kJ $mol^{-1}$

| | $[Phe+Na]^+$ | $[Phe+K]^+$ | > $[Phe+Ag]^+$ |
|---|---|---|---|
| TCID | 205.5[a] | 150.5[a] | +40 vs Gly[c] |
| equilibrium method | 187[b] | | |
| theory | 196[d]/201[e] | 140.8[a]/145[e] | 236[f]/270[g] |

[a] Ref 65. [b] Ref 68. [c] Ref 57. [d] 0 K binding enthalpies based on ref 65. [e] 0 K binding enthalpies based on ref ref 68. [f] 298 K binding enthalpy based on ref 67. [g] Present results.

For all three metal cations, the tridentate N/O/ring structure is calculated to be the most stable conformation.[18,57,59,65] All three metal cations are Lewis acids and would therefore be expected to have a similar binding behavior. The exact binding geometries do differ (see Table 2). For $K^+$ the bond distances are increased relative to $Na^+$, which can be rationalized by the larger size of $K^+$. The metal chelation bond distances for $Ag^+$ are not very different from $Na^+$.

This is also correlated to the higher binding enthalpy of Phe to $Ag^+$, resulting in the order of binding energies $Ag^+ > Na^+ > K^+$ (see Table 3). For $Ag^+$ the binding enthalpy has been calculated as 236 kJ $mol^{-1}$ at 298 K.[64] This was supported experimentally by the kinetic method,[66] which suggested that theory even underestimates the binding energy by ∼10 kJ $mol^{-1}$.[67] For $[Phe+Na]^+$ and $[Phe+K]^+$ the binding enthalpy is considerably lower even at 0 K, being approximated at ∼200 and 145 kJ $mol^{-1}$, respectively.

The carboxylic acid $\upsilon$(CO) band for $[Phe+Ag]^+$ is observed at 1718 $cm^{-1}$, whereas it was observed at 1750 $cm^{-1}$ for $[Phe+K]^+$.[38] This suggests a significant red-shift of 30 $cm^{-1}$ upon going from $K^+$ to $Ag^+$ as the chelating metal. This is in accordance with the M···O bond distance for $[Phe+Ag]^+$ (2.49 Å) which is reduced relative to $[Phe+K]^+$ (2.68 Å) (see Table 2). It is well-known that an increase in hydrogen bonding leads to a red-shift of $\upsilon$(CO) in peptides/proteins,[69] and a similar effect could reasonably be expected for decreasing metal chelation bond distances. The DFT calculations do not predict quite such a strong red-shift, but the agreement of calculation and experiment for $\upsilon$(CO) is well within expected margins for both of these systems.[39] Overall, the tridentate $[Phe+Ag]^+$ CS N/O/ring structure is strongly chelated, which explains its high stability relative to the bidentate SB O/O conformer and its low reactivity to $H_2O$ addition.[18]

**Zinc.** *Mass Spectrometry.* ESI of the solution containing phenylalanine and $ZnCl_2$ gives a deprotonated Zn Phe dimer complex, $[Zn+Phe_2-H]^+$ ($m/z$ 393 for $^{64}Zn$). It is believed that

(61) Piest, H.; von Helden, G.; Meijer, G. *J. Chem. Phys.* **1999**, *110*, 2010−2015.
(62) Oomens, J.; Moore, D. T.; Meijer, G.; von Helden, G. *Phys. Chem. Chem. Phys.* **2004**, *6*, 710−718.
(63) Marino, T.; Russo, N.; Toscano, M. *J. Phys. Chem. B* **2003**, *107*, 2588−2594.
(64) Jockusch, R. A.; Lemoff, A. S.; Williams, E. R. *J. Am. Chem. Soc.* **2001**, *123*, 12255−12265.
(65) Ruan, C.; Rodgers, M. T. *J. Am. Chem. Soc.* **2004**, *126*, 14600−14610.
(66) Lee, V. W.-M.; Li, H.; Lau, T.-C.; Guevremont, R.; Siu, K. W. M. *J. Am. Soc. Mass Spectrom.* **1998**, *9*, 760−766.
(67) Shoeib, T.; Siu, K. W. M.; Hopkinson, A. C. *J. Phys. Chem. A* **2002**, *106*, 6121−6128.
(68) Gapeev, A.; Dunbar, R. C. *Int. J. Mass Spectrom.* **2003**, *228*, 825−839.
(69) Barth, A.; Zscherp, C. *Q. Rev. Biophys.* **2002**, *35*, 369−430.

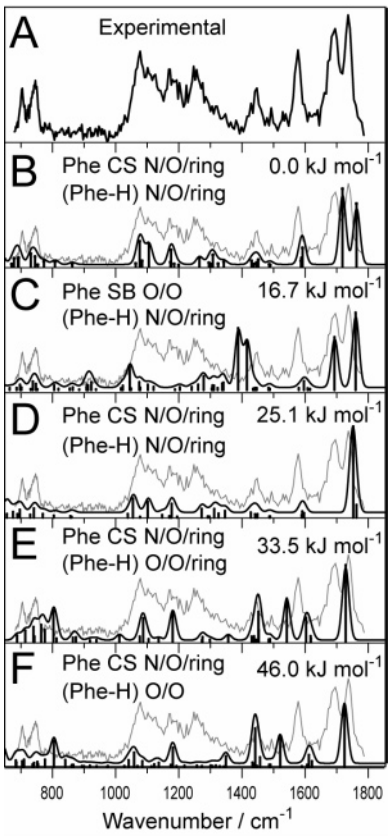


***Figure 3.*** (A) IR-MPD spectrum of $[Zn+Phe_2-H]^+$. Calculated spectra in ascending energy (B) Phe CS N/O/ring (Phe−H) N/O/ring, (C) Phe SB O/O (Phe−H) N/O/ring, (D) Phe CS N/O/ring (Phe−H) N/O/ring, (E) Phe CS N/O/ring (Phe−H) O/O/ring, and (F) Phe CS N/O/ring (Phe−H) O/O, overlaid with the experimental spectrum.

Zn(II) in protein catalytic sites facilitates the deprotonation of a bound water molecule,[42] and hence it is not totally surprising that an amino acid bound to Zn(II) is also deprotonated, such as observed here for $[Zn+Phe_2-H]^+$. Upon infrared excitation this complex fragments via two pathways: abundant loss of $H_2O$ (*m*/*z* 375) and some loss of Phe to yield the complex $[Zn+Phe-H]^+$ (*m*/*z* 228). Although the signal from the latter dissociation channel is fairly noisy, it does contain most of the spectral features of the water loss dissociation channel; both channels are simply added to give the total IR-MPD spectrum in Figure 3A.

*CS or SB Phe Ligand.* The deprotonated dimer complex $[Zn+Phe_2-H]^+$ has at least one Phe ligand with a de-protonated carboxylic acid terminus, which is referred to as (Phe−H) hereafter. For this ligand, the SB or CS question does not arise. The intact Phe ligand can either be in the CS or SB configuration. The nomenclature previously employed for $[Phe+Ag]^+$ is applied here to each of the two ligands Phe and (Phe−H). The lowest-energy calculated spectra and structures for $[Zn+Phe_2-H]^+$ are shown in increasing energy in Figures 3 and 4 (B to F). Since the conformation nomenclature is a bit long and ambiguous (compare B and D of Figure 3), the structures are simply referred to as structures B to F in the following discussion.

Only one of the shown calculated conformers includes a SB conformation on Phe, namely, structure C. Since (Phe−H) already has a carboxylate group, $\upsilon_{as}(CO_2^-)$ is no longer a diagnostic mode to identify the SB conformation of Phe in the $[Zn+Phe_2-H]^+$ complex. However, the umbrella modes of the $NH_3^+$ moiety, $\delta(NH_3^+)$, are still specifically diagnostic for the possible SB conformation of the Phe ligand. These modes should be seen with high intensity at ∼1400 $cm^{-1}$ (Figure 3C), while in the experimental spectrum, no band is observed at this position. The band at 1447 $cm^{-1}$ in the experimental spectrum could possibly be assigned as being the (blue-shifted) appearance of these SB modes, but the assignment of the 1447 $cm^{-1}$ feature as the OH bending mode, $\delta_{ip}(COH)$, of the CS configuration is a much better match for this feature. Thus, despite its relatively high stability (being the second most favored conformation), the SB conformation for Phe can be confidently excluded on the basis of the spectroscopic evidence.

*Assignment of Binding Geometry for $[Zn+Phe_2-H]^+$.* The theoretical study of $[Phe+Ag]^+$ yielded many possible conformations, of which only the five lowest-energy conformers are shown in Figure 2. For $[Zn+Phe_2-H]^+$ the number of putative binding geometries is even more daunting, and a complete search of the conformational space available to the complex is beyond the scope of this study. Nonetheless, the theoretical studies have consistently shown that the Phe and (Phe−H) ligands preferentially link via a N/O/ring tridentate geometry, in analogy to the results on $[Phe+Ag]^+$. Given the small size of the $Zn^{2+}$ ion and the high steric demands of the aromatic ligands, it might be expected that simultaneous 3-fold chelation of both ligands would be sterically unfavorable, so it is perhaps surprising to find that compact structures of this nature are substantially favored relative to more extended, lower-chelated alternatives. Two distinct conformers of this type are shown in B and D of Figure 4. They have in common a very similar 3-fold chelating binding geometry of the (Phe−H) ligand (see the structural parameters displayed in Figure 4). However, while both structures also show 3-fold chelating interaction of the Phe ligand with the metal ion, the binding geometries of this ligand are quite different in the two cases. For the lowest-energy structure, structure B, the Phe ligand is oriented so as to give a nearly tetrahedral geometry of the four Lewis-basic atoms (two O's and two N's). In contrast, conformer D gives a nearly square-planar geometry of these four basic atoms, and a lower metal−ring distance. Even though conformer D allows closer interaction of the benzene ring of Phe with the metal ion, this square-planar geometry overall incurs a significant energetic penalty of 25 kJ $mol^{-1}$ relative to the tetrahedral geometry of conformer B.

Of the many possible higher-energy, less chelated structures, two of the more favorable ones are shown in Figure 4, structures E and F. Both involve tridentate N/O/ring coordination of the Phe ligand, and 2-fold O/O chelation of the (Phe−H) ligand. In the case of structure E, some additional stabilization is provided by a distant chelation of the ring of the (Phe−H) ligand.

The calculated spectrum for structure B gives by far the best agreement with experiment. All the theoretical bands are reproduced with a reasonably faithful intensity pattern in the experimental spectrum, with a minor deviation around 1250−1300 $cm^{-1}$, where the relative band intensities differ. Given the nonlinearity of the IR-MPD mechanism, which has been discussed in detail,[48] as well as the difficulty of obtaining accurate relative intensities from calculation, the agreement of predicted spectrum B with experiment is remarkably close. The

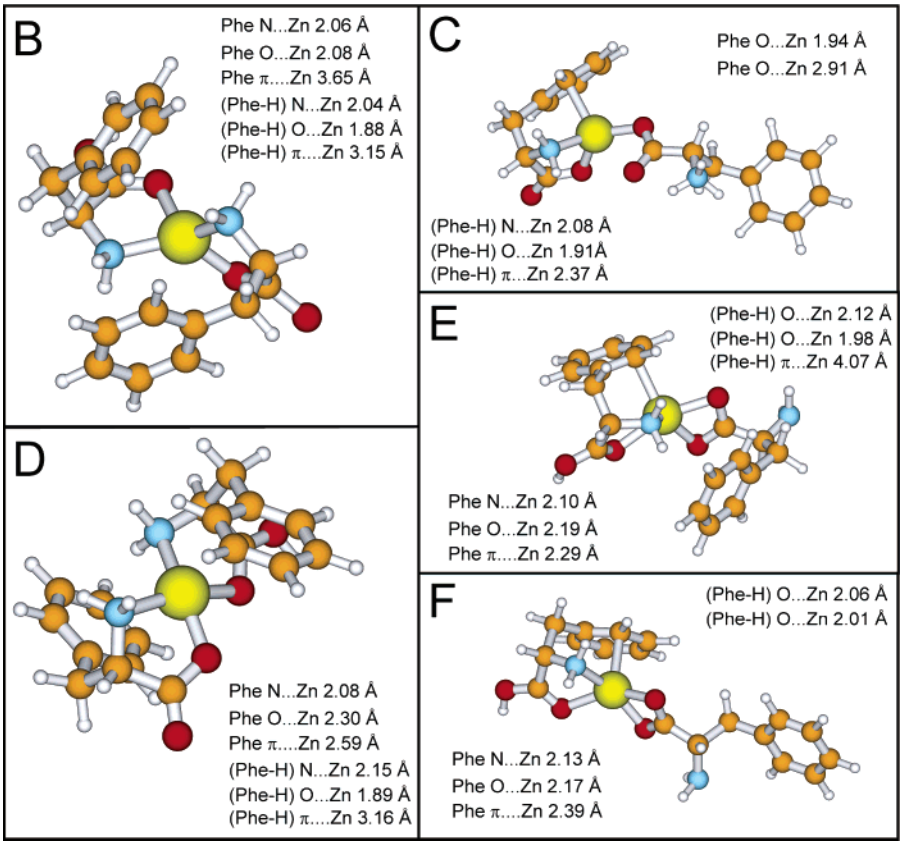


***Figure 4.*** Optimized structures: (B) Phe CS N/O/ring (Phe−H) N/O/ring, (C) Phe SB O/O (Phe−H) N/O/ring, (D) Phe CS N/O/ring (Phe−H) N/O/ring, (E) Phe CS N/O/ring (Phe−H) O/O/ring, and (F) Phe CS N/O/ring (Phe−H) O/O.

differences in the vibrational spectra between the calculated isomers are substantial, even between the rather similar structures B and D. Whereas structure B has two clearly distinguishable bands at ∼1700 $cm^{-1}$, only one major band is calculated in the case of structure D, giving a convincing basis for excluding structure D as a possible conformer. Structures E and F, which both display bidentate metal chelation through the (Phe−H) carboxylate group, predict an intense $\upsilon_{as}(CO_2^-)$ mode at ∼1530 $cm^{-1}$; however, no experimental band is seen at this position, allowing both of these conformers to be rejected. By analogy, carboxylate ligands in proteins are thought to favor monodentate binding to Zn if other ligands are available to bind.[70] Despite the many possible conformations for $[Zn+Phe_2-H]^+$, which could not all be explored here, the highly convincing fit that structure B gives to the experimental spectrum suggests that this conformer represents the predominant species.

*Preference for Tetrahedral Coordination.* In the absence of steric hindrance, one would expect the most highly chelated complex to be lowest in energy. Both structures B and D have a greater extent of chelation than any other structures that could be located, since both form tridentate chelation for each ligand. Judging by the relative bond lengths, conformer D has a stronger Zn $\pi$-bonding interaction with the aromatic Phe ligand, while conformer B has a tighter coordination to N and O; the O···Zn bond distance for Phe in particular is increased from 2.08 to 2.30 Å upon going from structure B to structure D. The energetic preference found here for structure B thus suggests that coordination of $Zn^{2+}$ to basic O and N atoms may give more stabilization than bonding to the $\pi$-cloud of the Phe side-chain. An analogy that supports this point of view is the well-known fact that $Zn^{2+}$ preferentially coordinates to N of histidine and O of glutamate in proteins, in comparison with the frequent cation-$\pi$ mode of binding found for alkali metal−amino acid interactions.[71,72]

Conformer B, with its tetrahedral-type $Zn^{2+}$ ligand chelation, is energetically favored relative to conformer D, with its square-planar-type chelation. The similarities to the natural world are striking. In proteins $Zn^{2+}$ has a strong preference for forming tetrahedral binding sites;[4,8] it is even used to make "designer" proteins with tetrahedral-coordinated sites.[6] A tetrahedral binding site would certainly be favored from a steric point of view, since the four ligands are thus farthest apart from one another. Due to the $d^{10}$ electronic configuration of $Zn^{2+}$, no geometry-related ligand field stabilization energy is available, and consequently no particular ligand coordination would be favored for orbital symmetry reasons.

*Spectral Assignment for [Phe(Phe−H)+Zn]$^+$.* The vibrational spectrum of $[Phe(Phe-H)+Zn]^+$ is quite well-resolved, and the close match with the calculated spectrum for conformer B enables an assignment of the vibrational modes (see Table 4). The C═O stretching modes at 1695 and 1736 $cm^{-1}$ are diagnostic for the binding of the Phe carboxylic acid and (Phe−H) carboxylate groups, respectively. These two modes are clearly separated, in marked contrast to the calculated spectrum of conformer D. The fact that the carboxylic acid $\upsilon$(C═O) of conformer D (calculated at ∼1760 $cm^{-1}$) is

(70) Ryde, U. *Biophys. J.* **1999**, *77*, 2777−2787.
(71) Dougherty, D. A. *Science* **1996**, *271*, 163−168.
(72) Ma, J. C.; Dougherty, D. A. *Chem. Rev.* **1997**, *97*, 1303−1324.

***Table 4.*** Assignment of the Observed Vibrational Bands of $[Phe(Phe-H)+Zn]^+$ in Figure 3A, Based on the Calculations for Structure B

| exptl ($cm^{-1}$) | calcd ($cm^{-1}$) | calcd intensity (km $mol^{-1}$) | assignment |
|---|---|---|---|
| 705 | 694 | 55 | Phe $\delta_{oop}$(OH) and aromatic $\delta_{oop}$(CH) |
| 746 | 732 | 81 | Phe aromatic $\delta_{oop}$(CH) |
| | 746 | 62 | (Phe−H) aromatic $\delta_{oop}$(CH) |
| 1078 | 1077 | 159 | (Phe−H) $\delta_{oop}(NH_2)$ |
| 1101 | 1106 | 145 | Phe $\delta_{oop}(NH_2)$ |
| 1168 | 1176 | 105 | Phe $\delta_{ip}$(COH)[a] |
| 1247 | 1266 | 56 | (Phe−H) $\upsilon_s(CO_2^-)$[b] |
| | 1309 | 73 | (Phe−H) aromatic $\upsilon$(CC) and $\delta_{ip}$(CH) |
| 1447 | 1431 | 36 | $\delta$(CH) |
| | 1446 | 25 | $\delta$(CH) |
| | 1452 | 43 | Phe $\delta_{ip}$(COH)[a] |
| 1577 | 1587 | 37 | $NH_2$ scissoring |
| | 1589 | 54 | $NH_2$ scissoring |
| | 1592 | 115 | $NH_2$ scissoring |
| 1695 | 1719 | 489 | Phe carboxylic acid $\upsilon$(CO) |
| 1736 | 1763 | 396 | (Phe−H) $\upsilon_{as}(CO_2^-)$[b] |

[a] $\delta_{ip}$(COH) always includes a large C−OH stretching component as well. [b] The (Phe−H) $\upsilon_{as}(CO_2^-)$ mode mainly consists of C═O stretching behavior on the uncoordinated CO.

calculated to be blue-shifted compared to the corresponding mode in conformer B (calculated at 1719 $cm^{-1}$) can be rationalized by the longer Phe O···Zn distance for conformer D, corresponding to less perturbation of the intrinsic carboxyl $\upsilon$(C═O) near 1800 $cm^{-1}$. The agreement of the observed spectrum with the predictions for both B and D are entirely satisfactory over the range below 1650 $cm^{-1}$, but there are no definitive diagnostic features in this range that would confirm assignment to one or the other structure.

## Conclusions

The present study has shown that infrared spectroscopy in combination with DFT calculations can yield valuable information about the coordination of transition metals linked to amino acids in the gas phase. For systems of this size and complexity, these spectra are notable for the number of clearly identifiable peaks resolved in the IR-MPD spectra. The close matches with the DFT-calculated spectra of the most stable geometries make a solid link between these information-rich spectra and interesting structural features of the molecules. In correlation with computed spectra of possible isomeric structures, IR-MPD of $[Phe+Ag]^+$ definitely confirms a tridentate charge-solvated (CS) binding pattern for the room-temperature ions and strongly indicates that the CS N/O/ring structure is favored relative to the alternative CS N/OH/ring structure, in agreement with the theoretical expectation based on the relative stabilities of these two conformers. Compared to the alkali metals $Na^+$ and $K^+$, $Ag^+$ is more tightly bound to Phe, which explains the low reactivity of $[Phe+Ag]^+$ to water addition.[18]

In the zinc case, the deprotonated dimer complex $[Zn+Phe_2-H]^+$ involving the +2 oxidation state of Zn was investigated. A tightly coordinated N/O/ring structure is calculated to be the lowest-energy conformer and gives a close fit to the experimental spectrum; this structure has a tetrahedral-type core with respect to the four O and N coordination sites, which is energetically favored relative to the square-planar-type geometry (conformer D). It is well-known that $Zn^{2+}$ has a strong prevalence of tetrahedral binding conformations in proteins, which can be rationalized by the absence of a ligand field stabilization energy.[9] The present results are in accord with this generalization.

Even for the out-of-plane (and sometimes anharmonic) vibrations the agreement between experiment and theory is remarkably close, and this spectral region holds much potential for the differentiation of conformers. The sensitivity of IR spectroscopy to variations in metal−ligand coordination geometries makes the technique particularly useful in the structural elucidation of transition metal−biomolecule complexes that serve as gas-phase mimics of reactive centers of proteins; thus, the inherent structures of such complexes can be studied in the absence of solvent or other environmental effects.

**Acknowledgment.** FOM is financially supported by the Nederlandse Organisatie voor Wetenschappelijk Onderzoek (NWO). We gratefully acknowledge the skillful assistance by the FELIX staff, in particular Drs. B. Redlich and A. F. G. van der Meer. Construction and shipping of the FTICR-MS was made possible with funding from the National High Field FT-ICR Facility (Grant CHE-9909502) at the National High Magnetic Field Laboratory, Tallahassee, FL, which also supported travel for R.C.D. We thank Professors J. R. Eyler and A. G. Marshall for their collaboration with this project. R.C.D. acknowledges the support of the donors of the Petroleum Research Fund, administered by the American Chemical Society.

**Supporting Information Available:** Complete ref 55. This material is available free of charge via the Internet at http:// pubs.acs.org.

JA0549291